

The effect of composition on pressure-induced devitrification in metallic glasses

Qiaoshi Zeng, Wendy L. Mao, Hongwei Sheng, Zhidan Zeng, Qingyang Hu et al.

Citation: *Appl. Phys. Lett.* **102**, 171905 (2013); doi: 10.1063/1.4803539

View online: <http://dx.doi.org/10.1063/1.4803539>

View Table of Contents: <http://apl.aip.org/resource/1/APPLAB/v102/i17>

Published by the [American Institute of Physics](http://www.aip.org).

Additional information on *Appl. Phys. Lett.*

Journal Homepage: <http://apl.aip.org/>

Journal Information: http://apl.aip.org/about/about_the_journal

Top downloads: http://apl.aip.org/features/most_downloaded

Information for Authors: <http://apl.aip.org/authors>

ADVERTISEMENT

An advertisement banner for Applied Physics Letters. It features a dark orange background with a lighter orange gradient at the bottom. On the left, there is a white envelope icon. The text 'AIP | Applied Physics Letters' is prominently displayed in white. Below this, a yellow box contains the text 'Accepting Submissions in Biophysics and Bio-Inspired Systems' and a 'Submit Today' button. On the right, the AIP Publishing logo is shown in a yellow-bordered box.

AIP | Applied Physics Letters

Accepting Submissions in
Biophysics and Bio-Inspired Systems

Submit Today

AIP
Publishing

The effect of composition on pressure-induced devitrification in metallic glasses

Qiaoshi Zeng,^{1,2,3,4,a)} Wendy L. Mao,^{1,2,4,a)} Hongwei Sheng,⁵ Zhidan Zeng,^{1,2,6} Qingyang Hu,⁵ Yue Meng,⁷ Hongbo Lou,⁴ Fang Peng,^{3,8} Wenge Yang,³ Stanislav V. Sinogeikin,⁷ and Jian-Zhong Jiang⁴

¹Geological and Environmental Sciences, Stanford University, Stanford, California 94305, USA

²Photon Science and Stanford Institute for Materials and Energy Sciences, SLAC National Accelerator Laboratory, Menlo Park, California 94025, USA

³HPSynC, Geophysical Laboratory, Carnegie Institution of Washington, 9700 South Cass Avenue, Argonne, Illinois 60439, USA

⁴International Center for New-Structured Materials, Zhejiang University and Laboratory of New-Structured Materials, Department of Materials Science and Engineering, Zhejiang University, Hangzhou 310027, People's Republic of China

⁵School of Physics, Astronomy & Computational Sciences, George Mason University, Fairfax, Virginia 22030, USA

⁶Center for High Pressure Science and Technology Advanced Research (HPSTAR), Shanghai 201203, China

⁷HPCAT, Geophysical Laboratory, Carnegie Institution of Washington, 9700 South Cass Avenue, Argonne, Illinois 60439, USA

⁸Institute of Atomic and Molecular Physics, Sichuan University, Chengdu 610065, China

(Received 28 March 2013; accepted 17 April 2013; published online 30 April 2013)

Long-range topological order (LRTO) was recently revealed in a $\text{Ce}_{75}\text{Al}_{25}$ metallic glass (MG) by a pressure-induced devitrification (PID) at 300 K. However, what compositions may have PID and an understanding of the physical and chemical controls behind PID are still not clear. We performed *in situ* high pressure x-ray diffraction measurements on $\text{Ce}_x\text{Al}_{1-x}$ ($x = 65, 70, \text{ and } 80$ at. %) MGs. Combining our experimental results and simulations, we found PID is very sensitive to compositions and can only exist over narrow compositional ranges. These results provide valuable guidance for searching for PID in MGs. © 2013 AIP Publishing LLC [<http://dx.doi.org/10.1063/1.4803539>]

Metallic glass (MG), as a new member of the glass family, has stimulated widespread research interest due to their unique technological promise for practical applications, and also scientific importance in understanding glass by providing new model systems. Compared to conventional glass, MG with non-directional metallic bonding generally requires faster cooling rates over a large range of 10^6 to 10^{-1} K/s depending on the composition.¹ Glass, crystal, and even quasicrystal² phases can form by controlling the melt-quenching rates in metallic alloy systems. It has been established that nominally “disordered” glass structure still has short-range order (SRO) of the nearest-neighbor atoms or even medium-range order (MRO) on length scale longer than the nearest neighbor to several nm.³ Whether a more ordered glass state can exist in melt-quenched MGs is a very intriguing question. Recently, Zeng *et al.* revealed a long-range topological order (LRTO) in a $\text{Ce}_{75}\text{Al}_{25}$ MG by a pressure-induced devitrification (PID) into a single crystal with fixed crystallographic orientation at room temperature.⁴ The result implies a more ordered state may extensively exist in some MGs and that PID plays a unique role in manifesting the otherwise invisible LRTO. Thus, PID has exciting potential in the search for more “ordered” glasses in MGs, which can be expected to overcome the principal drawback of standard glasses with lower fragility.⁵

It is well known that glass is thermodynamically metastable, and thus prefers to devitrify when provided with enough energy to overcome the kinetic barrier to crystallization. In general, when heated, glasses devitrify into random polycrystalline aggregates via the nucleation and growth process, in which case direct correlation between the glassy and crystalline structures is difficult to obtain.⁶ Pressure offers an alternative route to induce amorphization or devitrification. PID has been reported in a few non-metallic amorphous materials with open network structures, e.g., H_2O ,⁷ Si,⁸ Ge,⁹ Se,¹⁰ ZnCl_2 ,¹¹ $\text{Al}_2\text{O}_3\text{-Y}_2\text{O}_3$,¹² $\text{Ge}_2\text{Sb}_2\text{Te}_5$.¹³ Although minute amount of nano-crystal devitrification in MGs induced by severe deformation was reported,¹⁴ it actually involves very strong thermal effects¹⁵ and causes damage to the incipient structure of the MG matrix. Thus, compared to traditional open network glasses, it was suggested that it would be very difficult for pure PID to occur in MGs due to the nondirectional, densely packed atomic structure (coordination numbers up to 12–14) and the very low atomic mobility of these materials under hydrostatic high pressures.⁹

Thus, it is very surprising to observe a devitrification from the entire bulk $\text{Ce}_{75}\text{Al}_{25}$ MG sample at high pressure and room temperature. When the $\text{Ce}_{75}\text{Al}_{25}$ MG sample was compressed under hydrostatic pressure and at 300 K, the mismatch between Ce and Al will be significantly diminished due to the pressure-induced delocalization of the 4f electron of Ce and the large differences between bulk moduli of Ce ($K_0 \sim 20$ GPa)¹⁶ and Al ($K_0 \sim 73$ GPa),¹⁷ eventually the pressure brings Ce and Al within the Hume-Rothery limits for

^{a)}Authors to whom correspondence should be addressed. Electronic addresses: qiaoshiz@stanford.edu and wmao@stanford.edu

substitutional solid solution alloying and causes PID,^{4,18} basically no long-range atomic diffusion is necessarily involved, and as a result the underlying LRTO is manifested by the formation of a giant single crystal with fixed crystallographic orientation from the entire bulk sample.⁴ The PID product of $\text{Ce}_{75}\text{Al}_{25}$ MG is a substitutional solid solution alloy.¹⁸ Solid solution alloys can generally exist over a wide compositional range. In addition, recent work reveals that the solvent components dominate the properties of MGs and usually show very similar properties over different compositions,¹⁹ thus this kind of PID is expected in Ce-based Ce-Al MGs over the entire compositional range ($C_{\text{Ce}} > 50\%$) as well. However, Sheng *et al.* surprisingly reported that no PID was observed up to 30 GPa in $\text{Ce}_{55}\text{Al}_{45}$ MG.²⁰ These results raise some intriguing questions: What compositions of MGs display PID and why? And what are the physical and chemical controls behind PID? Answering these questions will be an important guide for searching for more glass systems with PID and will shed new light on the investigation of glass structure.

To determine the effect of composition on PID, a systematic investigation of the Ce-based Ce-Al system is required. We used *in situ* high pressure XRD to monitor possible PID in three $\text{Ce}_x\text{Al}_{100-x}$ ($x = 65, 70$, and 80 at. %) MGs at 300 K (see Figure 1 for the compositions investigated in the Ce-Al phase diagram²¹). Then, the effect of composition on PID in MGs was interpreted based on the molecular dynamics (MD) calculations and insight from the elastic instability mechanism.^{22,23} $\text{Ce}_x\text{Al}_{100-x}$ ($x = 70$ and 65 at. %) MGs were prepared by single-roller melt-spinning into ribbons with a thickness of approximately $20 \mu\text{m}$ and a width of 1 mm. Since $\text{Ce}_{80}\text{Al}_{20}$ MG is difficult to prepare by melt-spinning with its marginal glass forming ability, a thinner film with a thickness of approximately $5 \mu\text{m}$ was prepared by single-target magnetron-sputtering method. The fully amorphous structure of the as-prepared samples was characterized

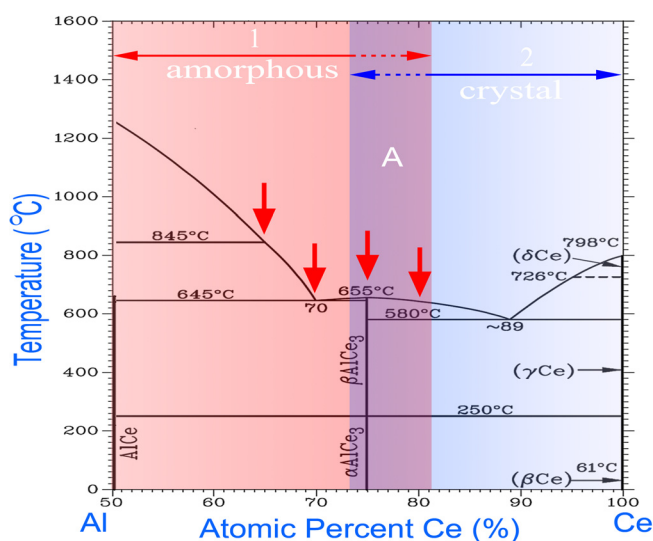


FIG. 1. The phase diagram for the Ce-based Ce-Al system at ambient pressure. The red arrows indicate the compositions we investigated using *in situ* high pressure XRD measurements in this study or previously (see Ref. 4). Purple region A (the overlap of the regions of ambient pressure glass formation region 1) and high pressure solid solution formation (region 2)) is the compositional range predicted to have possible PID.

by synchrotron XRD. The *in situ* high pressure XRD experiments were performed in a symmetric diamond anvil cell (DAC) with helium as the pressure medium at beamlines 16-BM-D and 16-ID-B of the High Pressure Collaborative Access Team (HPCAT), Advanced Photon Source (APS), Argonne National Laboratory (ANL) and also at beamline 12.2.2, Advanced Light Source (ALS), Lawrence Berkeley National Laboratory (LBNL).

Figure 2 shows the *in situ* high pressure XRD patterns of $\text{Ce}_x\text{Al}_{100-x}$ ($x = 65, 70$, and 80 at. %) MGs. The main peaks shift to higher Q values with increasing pressure as a result of densification. In repeated experiments, we found the lower Ce content MGs ($\text{Ce}_{65}\text{Al}_{35}$ and $\text{Ce}_{70}\text{Al}_{30}$) remained fully amorphous over the entire pressure range as indicated by the smooth patterns and absence of sharp Bragg peaks, which is consistent with the reported results for $\text{Ce}_{55}\text{Al}_{45}$ MG.²⁰ However, devitrification into a face-centered cubic solid solution phase was observed in the higher Ce content MG $\text{Ce}_{80}\text{Al}_{20}$ around 37 GPa, which is similar to the previous results in $\text{Ce}_{75}\text{Al}_{25}$ MG.¹⁸ Unlike the line compounds in the ambient pressure phase diagram which have a fixed composition and an ordered distribution of Ce and Al on lattice sites (Figure 1), this solid solution alloy is supposed to be able to exist over a range of compositions with Ce and Al randomly distributed on lattice sites. Although the compositions of $\text{Ce}_x\text{Al}_{100-x}$ ($x = 65, 70, 75$, and 80 at. %) MGs have only small 5% differences in concentrations, no PID was observed up to 42 GPa in MGs with x less than 75%, which indicates the PID must be very sensitive to composition.

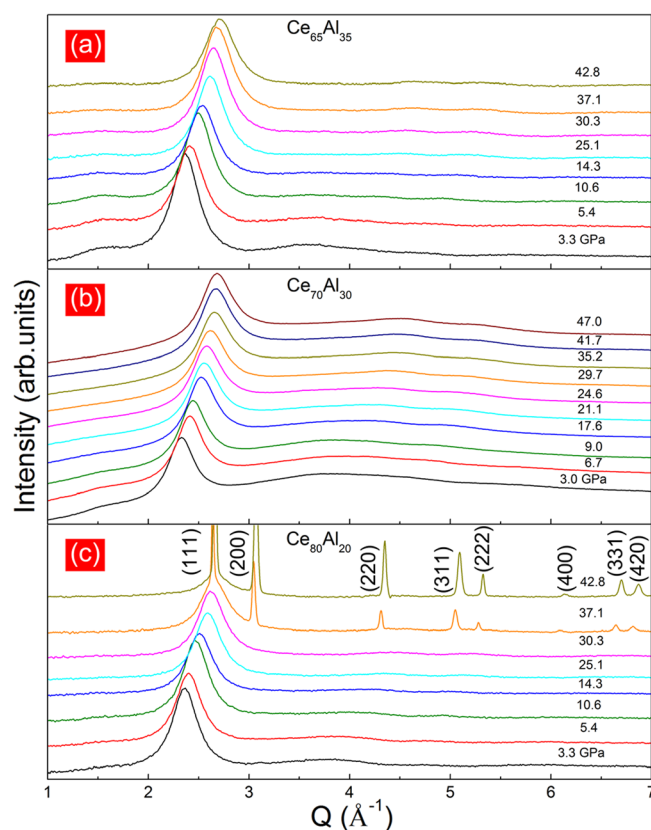


FIG. 2. *In situ* high pressure XRD patterns for, (a) $\text{Ce}_{65}\text{Al}_{35}$, (b) $\text{Ce}_{70}\text{Al}_{30}$, and (c) $\text{Ce}_{80}\text{Al}_{20}$ MGs. $\text{Ce}_{65}\text{Al}_{35}$ and $\text{Ce}_{80}\text{Al}_{20}$ MGs were loaded in the same DAC.

What then is the mechanism of the PID? According to Hume-Rothery rules, atomic size difference is a very important factor for solid solution formation. When there is a large difference in atomic size between solute and solvent atoms, then the solubility will be limited by the stress induced by the atomic radii mismatch; if the solute concentration exceeds a critical value, the stress accumulated will cause the elastic destabilization of the solid solution crystal lattice, i.e., an amorphous structure is then favored over a solid solution crystal during rapid quenching of a molten alloy, here called an elastic instability mechanism.^{22–24} Thus, the atomic size difference is verified to be a key factor for MG formation²⁵ and plays a dominant role in binary MG formation.^{22–24,26}

Li and Johnson investigated solid vitrification using MD simulations and found that solid vitrification could occur if the solute concentration and solute-solvent atomic size difference are both sufficiently large.²³ So far, there is no universal model which can predict the glass forming ability in MGs.²⁴ However, considering the dominant factors in a binary system, both the atomic size difference and solute concentration, a simple relationship to guide the MG synthesis in binary alloy systems by traditional melt-quenching to room temperature has been semi-empirically established^{22,26} as: $C_b^*|(r_b/r_a)^3 - 1| \approx 1$ (1), where C_b^* is the critical minimum solute concentration, r_a and r_b are the atomic radii of the solvent and solute, respectively. For the Ce-based Ce-Al binary system, according to Eq. (1) the critical minimum concentration of Al, C_{Al}^* , required for the formation of a MG is about 19 at. % at ambient conditions. We do find a very close composition, $Ce_{80}Al_{20}$, is the critical glass formation composition using melt-spinning, which is very consistent with the prediction in a meticulous simulation work for binary systems.²⁴

High pressure is a powerful tool for tuning the atomic radius. Although Ce has a much bigger atomic radius (18%) than Al at ambient conditions, pressure induced delocalization of the $4f$ electron results in a large volume collapse in the Ce atoms. Additionally, the bulk modulus of Al is approximately three times larger than that of Ce. The atomic radii of elements with smaller bulk moduli usually decrease faster during compression,²⁷ thus the atomic radii difference between the solvent Ce and solute Al is markedly reduced by pressure. The term $|(r_{Al}/r_{Ce})^3 - 1|$ in Eq. (1) will approach to zero during compression, resulting in the increase of C_{Al}^* . With increasing pressure, for a given composition, the real solute concentration C_{Al} may then fall below C_{Al}^* , i.e., C_{Al} is no longer sufficiently large to stabilize the glass structure, and the sample will prefer to devitrify into a solid solution crystal. As a polymorphic process, only a small deviation from the amorphous packing structure should be sufficient for the devitrification (see the schematic illustration in Figure 3).

Due to the interaction between Al and Ce, the existing high pressure data of atomic radii of pure Ce and Al cannot be directly used for the Ce-Al system.^{18,20} By using MD simulations, we can determine the pressure dependence of the average atomic radii of Ce and Al in a Ce based Ce-Al glass system (half of the first neighbour distance in their partial pair distribution functions),⁴ and the pressure dependence of the C_{Al}^* required for the Ce-Al MG devitrification

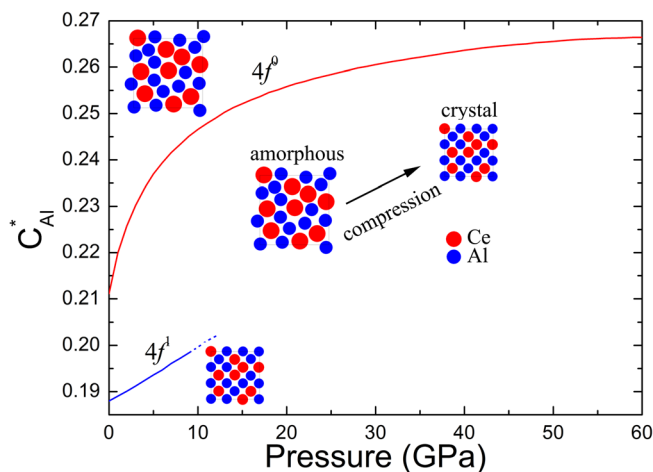


FIG. 3. The critical solute (Al) concentration C_{Al}^* in Ce-based Ce-Al MG required for devitrification under high pressure.

(or formation) can then be readily calculated by Eq. (1) (Figure 3). For a given composition, there is a critical pressure for glass devitrification. Since the atomic radii cannot be indefinitely reduced with increasing pressure, the pressure dependence of C_{Al}^* eventually saturates at a finite value. This means that high pressure can only induce devitrification over a limited compositional region in the Ce-Al MG system. At ambient pressure, the $4f$ electron of Ce is completely localized, and C_{Al}^* is about 19%. A Ce-based Ce-Al MG can relatively easily form by melt-quenching at ambient pressure when the C_{Al} is larger than 19%. When the Ce atom is compressed, delocalization of the $4f$ electron occurs. For the pure itinerant $4f$ electronic state of Ce, C_{Al}^* saturates at about 27% under high pressure, which means when pressure is high enough PID can occur in Ce-based Ce-Al MGs with the $C_{Al} < 27\%$. Considering the glass forming region (Marked as region 1 in Figure 1), $C_{Al} > 19\%$, thus PID can be observed only over the narrow compositional region with $19\% < C_{Al} < 27\%$ in Ce-based Ce-Al MGs. These predictions for compositional range are completely consistent with the experimental result that no PID was observed in $Ce_{70}Al_{30}$, $Ce_{65}Al_{35}$, and $Ce_{55}Al_{45}$ MGs with $C_{Al} > 27\%$; meanwhile PID was observed at ~ 25 GPa in $Ce_{75}Al_{25}$ MG^{4,18} and ~ 37 GPa in $Ce_{80}Al_{20}$ MG with $19\% < C_{Al} < 27\%$. This model provides us with a very simple picture for predicting possible compositions for PID; however, it should be noted that many other constraints of glass formation besides atomic radii difference, e.g., electronegativity difference,¹⁸ electronic interactions between atoms,²⁸ experimental cooling speed,²⁴ etc. may also be able to shift the compositional region of PID or alter its width. In addition, besides the slight uncertainty in Eq. (1),²⁴ PID is a kinetic process, thus the pressure observed for PID in each experiment may be different from the predicted value in Figure 3. The properties of MGs are also very sensitive to their thermal histories, and therefore the actual critical pressure of PID may shift between different samples with the same compositions (e.g., we observe some fluctuations of more than 10 GPa in the critical pressures for PID in $Ce_{75}Al_{25}$ MG samples with different thermal histories). That may explain why the pressure of PID in $Ce_{80}Al_{20}$ MG synthesized by magnetron-sputtering is ~ 37 GPa, which is much

higher than the predicted value. Combining the experimental observations and MD simulations, it can be concluded that although high pressure can significantly reduce the radii difference between Ce and Al, PID does not occur in the Ce-based Ce-Al MGs until the solute (Al) concentration falls within the narrow region A marked in Figure 1.

In summary, based on *in situ* high pressure XRD experimental results in the $\text{Ce}_x\text{Al}_{100-x}$ ($x = 80, 75$ (Ref. 4), 70, 65, and 55 (Ref. 20) at. %) MGs, MD simulations and the elastic instability mechanism, we conclude that high pressure can only induce devitrification in a binary MG if it meets two conditions: (1) the larger atom is more compressible than the smaller one (pressure can then decrease the atomic radii difference) and (2) the solute concentration must be located within a narrow region below the saturated critical value under high pressure and above the critical value required for glass formation at ambient pressure. These criteria could also be extended more generally to multicomponent systems by $\sum C_i |(r_i/r_a)^3 - 1| \approx 1$, where r_i and r_a are the atomic radii of the solute and solvent, respectively.²⁹ The effect of composition on PID in MGs addressed here provides new insight and guidance for searching for PID in other MG systems, and sheds light on the investigation of some fundamental questions in glass structure by linking the glass structure with crystal structure directly via PID.

We thank Dr. Arturas Vailionis from the Geballe Laboratory for Advanced Materials, Stanford University for his assistance with the ambient XRD measurements. This research was supported by DOE and DE-AC02-76SF00515, and also as part of EFree, an Energy Frontier Research Center funded by the U.S. Department of Energy (DOE), Office of Science, Office of Basic Energy Sciences (BES) under Award No. DE-SC0001057. Using of the HPCAT facility is supported by DOE-NNSA under Award No. DE-NA0001974 and DOE-BES under Award No. DE-FG02-99ER45775, with partial instrumentation funding by NSF. Use of the gas loading system at GSECARS was supported by NSF (EAR-0622171, EAR 06-49658, and EAR 10-43050), DOE (DE-FG02-94ER14466), and COMPRES. APS is supported by DOE-BES, under Contract No. DE-AC02-06CH11357. The ALS is supported by the Director, Office of Science, DOE-BES under Contract No. DE-AC02-05CH11231. The effort from Zhejiang University was supported by the Zhejiang University–Helmholtz

Cooperation Fund and the Basic Research Program of China (2012CB825700).

- ¹A. L. Greer, *Science* **267**, 1947 (1995).
- ²D. Shechtman, I. Blech, D. Gratias, and J. W. Cahn, *Phys. Rev. Lett.* **53**, 1951 (1984).
- ³H. W. Sheng, W. K. Luo, F. M. Alamgir, J. M. Bai, and E. Ma, *Nature* **439**, 419 (2006).
- ⁴Q. S. Zeng, H. W. Sheng, Y. Ding, L. Wang, W. G. Yang, J. Z. Jiang, W. L. Mao, and H. K. Mao, *Science* **332**, 1404 (2011).
- ⁵J. Haines, C. Levelut, A. Isambert, P. Hebert, S. Kohara, D. A. Keen, T. Hammouda, and D. Andrault, *J. Am. Chem. Soc.* **131**, 12333 (2009).
- ⁶M. B. Kruger and R. Jeanloz, *Science* **249**, 647 (1990).
- ⁷O. Mishima and H. E. Stanley, *Nature* **396**, 329 (1998).
- ⁸S. Minomura, *J. Phys. (Paris)* **42**, 181 (1981); P. F. McMillan, *J. Mater. Chem.* **14**, 1506 (2004).
- ⁹M. H. Bhat, V. Molinero, E. Soignard, V. C. Solomon, S. Sastry, J. L. Yarger, and C. A. Angell, *Nature* **448**, 787 (2007).
- ¹⁰H. Z. Liu, L. H. Wang, X. H. Xiao, F. De Carlo, J. Feng, H. K. Mao, and R. J. Hemley, *Proc. Natl. Acad. Sci. U.S.A.* **105**, 13229 (2008).
- ¹¹C. H. Polisky, L. M. Martinez, K. Leinenweber, M. A. VerHelst, C. A. Angell, and G. H. Wolf, *Phys. Rev. B* **61**, 5934 (2000).
- ¹²S. Aasland and P. F. McMillan, *Nature* **369**, 633 (1994).
- ¹³Y. Q. Cheng, M. Xu, H. W. Sheng, Y. Meng, X. D. Han, and E. Ma, *Appl. Phys. Lett.* **95**, 131904 (2009); M. Krbal, A. V. Kolobov, J. Haines, P. Fons, C. Levelut, R. Le Parc, M. Hanfland, J. Tominaga, A. Pradel, and M. Ribes, *Phys. Rev. Lett.* **103**, 115502 (2009).
- ¹⁴H. Chen, Y. He, G. J. Shiflet, and S. J. Poon, *Nature* **367**, 541 (1994); L. Sun, W. K. Wang, D. W. He, W. H. Wang, Q. Wu, X. Y. Zhang, Z. X. Bao, and Q. Zhao, *Appl. Phys. Lett.* **76**, 2874 (2000).
- ¹⁵J. J. Lewandowski and A. L. Greer, *Nature Mater.* **5**, 15 (2006).
- ¹⁶J. Staun Olsen, L. Gerward, U. Benedict, and J.-P. Itié, *Phys. B* **133**, 129 (1985).
- ¹⁷A. K. Singh, H.-P. Liermann, Y. Akahama, and H. Kawamura, *J. Appl. Phys.* **101**, 123526 (2007).
- ¹⁸Q. S. Zeng, Y. Ding, W. L. Mao, W. Luo, A. Blomqvist, R. Ahuja, W. Yang, J. Shu, S. V. Sinogeikin, Y. Meng, D. L. Brewster, J. Z. Jiang, and H. K. Mao, *Proc. Natl. Acad. Sci. U.S.A.* **106**, 2515 (2009).
- ¹⁹D. Ma, A. D. Stoica, X. L. Wang, Z. P. Lu, B. Clausen, and D. W. Brown, *Phys. Rev. Lett.* **108**, 085501 (2012).
- ²⁰H. W. Sheng, H. Z. Liu, Y. Q. Cheng, J. Wen, P. L. Lee, W. K. Luo, S. D. Shastri, and E. Ma, *Nature Mater.* **6**, 192 (2007).
- ²¹T. B. Massalski, H. Okamoto, P. R. Subramanian, and L. Kacprzak, *Binary Alloy Phase Diagrams*, 2nd ed. (ASM International, Ohio, 1990).
- ²²T. Egami and Y. Waseda, *J. Non-Cryst. Solids* **64**, 113 (1984).
- ²³M. Li and W. L. Johnson, *Phys. Rev. Lett.* **70**, 1120 (1993).
- ²⁴P. Jalali and M. Li, *Phys. Rev. B* **71**, 014206 (2005).
- ²⁵A. Inoue, *Acta Mater.* **48**, 279 (2000); D. B. Miracle, *Nature Mater.* **3**, 697 (2004).
- ²⁶T. Egami, *Mater. Sci. Eng., A* **226–228**, 261 (1997).
- ²⁷Y. Z. Guo and M. Li, *J. Appl. Phys.* **108**, 113510 (2010).
- ²⁸Y. Q. Cheng, E. Ma, and H. W. Sheng, *Phys. Rev. Lett.* **102**, 245501 (2009).
- ²⁹R. D. Sa Lisboa, C. Bolfarini, W. J. F. Botta, and C. S. Kiminami, *Appl. Phys. Lett.* **86**, 211904 (2005).